remote sensing

Supplementary Materials

A Sequential Autoencoder for Teleconnection Analysis

Jiena He and J. Ronald Eastman

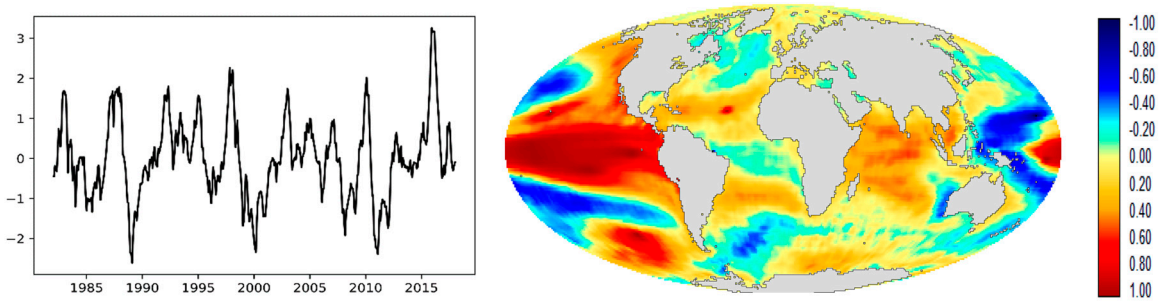

(a) (b)

Figure S1. (a) EOT Component 1; (b) EOT Component 1 loading image

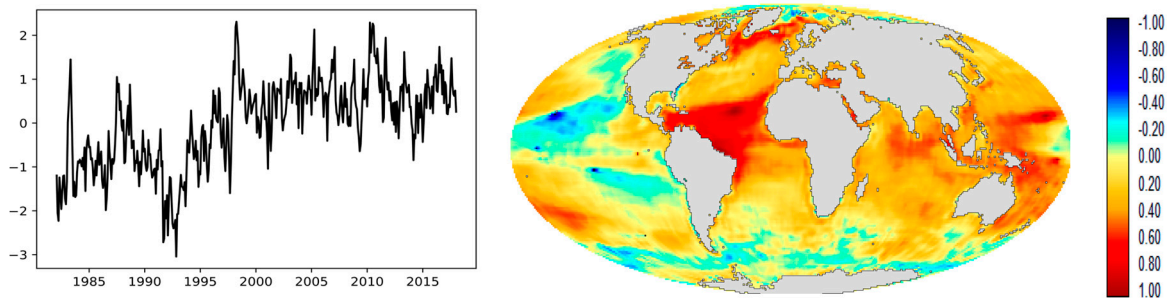

(a) (b)

Figure S2. (a) EOT Component 2; (b) EOT Component 2 loading image

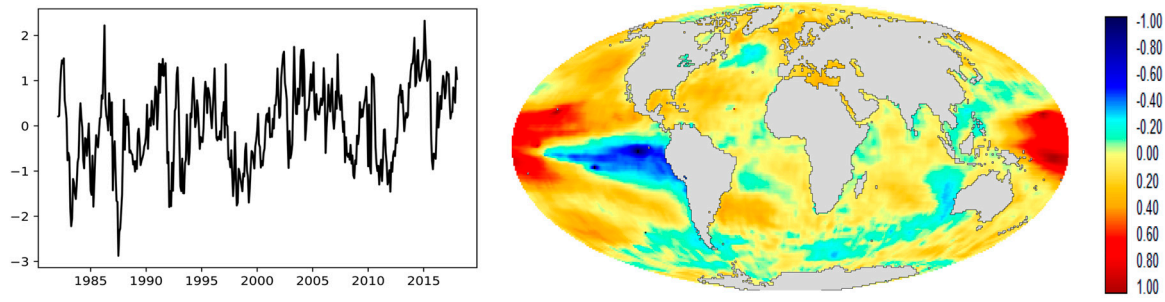

(a) (b)

Figure S3. (a) EOT Component 3; (b) EOT Component 3 loading image

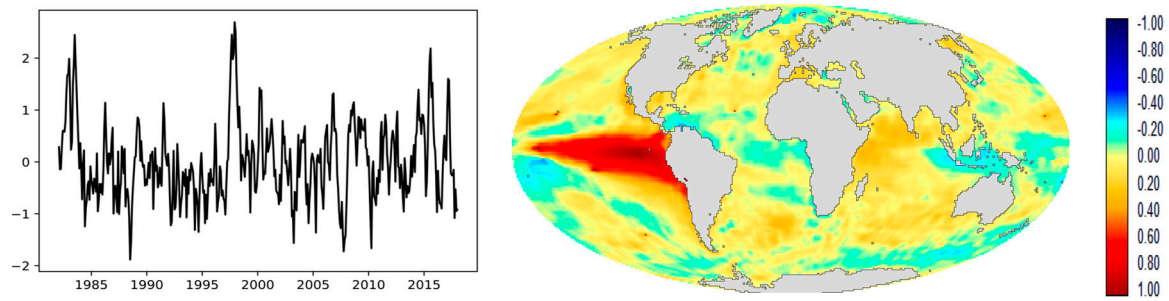

(a) (b)

Figure S4. (a) EOT Component 4; (b) EOT Component 4 loading image

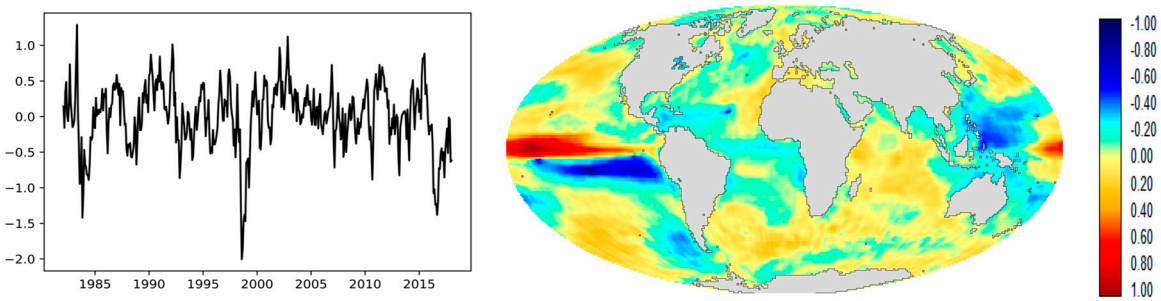

(a) (b)

Figure S5. (a) EOT Component 5; (b) EOT Component 5 loading image

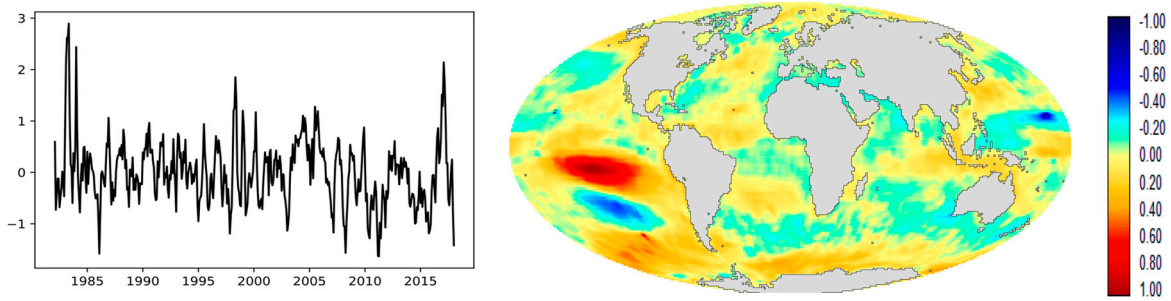

(a) (b)

Figure S6. (a) EOT Component 6; (b) EOT Component 6 loading image

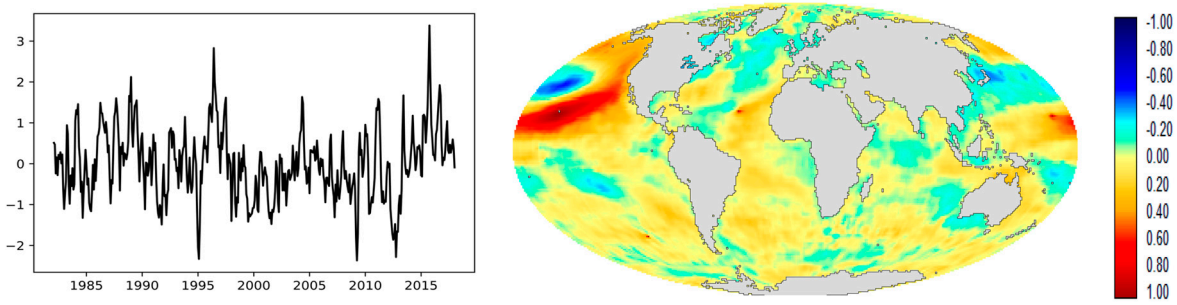

(a) (b)

Figure S7. (a) EOT Component 7; (b) EOT Component 7 loading image

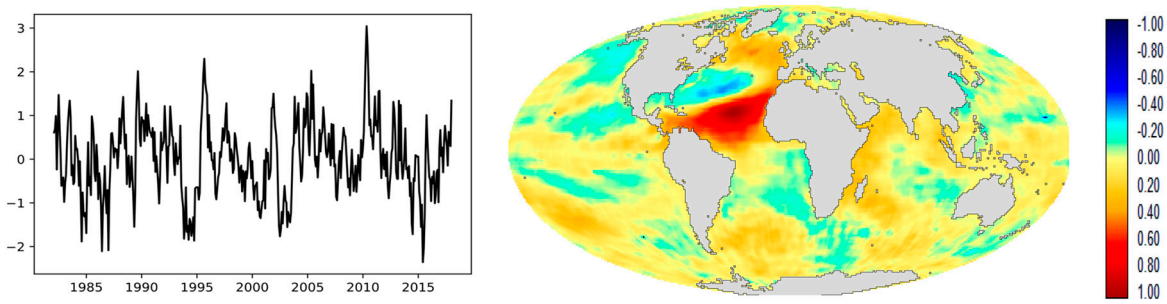

(a) (b)

Figure S8. (a) EOT Component 8; (b) EOT Component 8 loading image

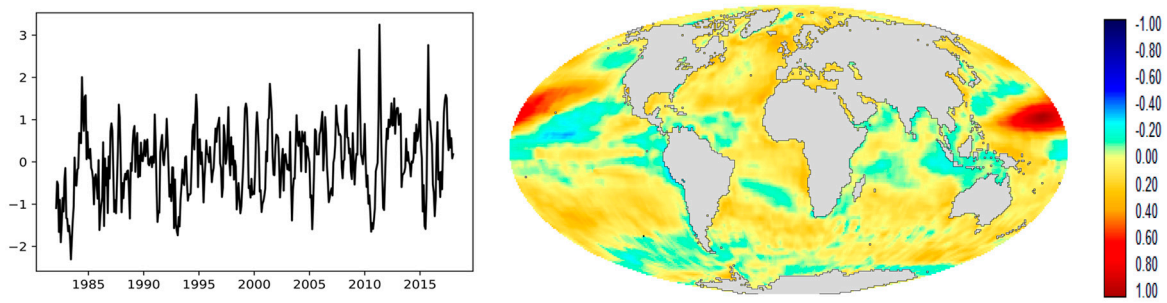

(a) (b)

Figure S9. (a) EOT Component 9; (b) EOT Component 9 loading image

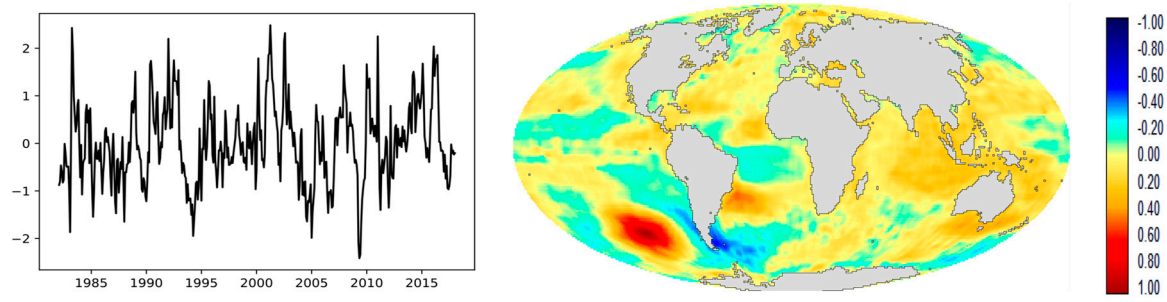

(a) (b)

Figure S10. (a) EOT Component 10; (b) EOT Component 10 loading image

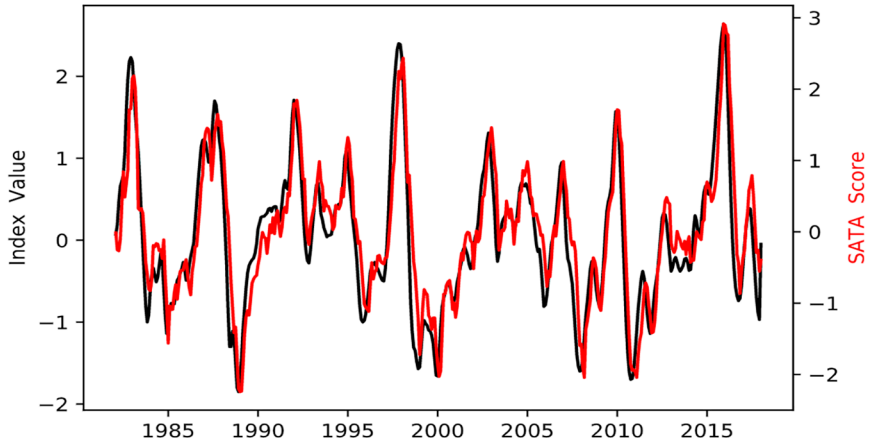

Figure S11. Comparison of the component score for SC1 (red) with the Oceanic Nino Index (black).

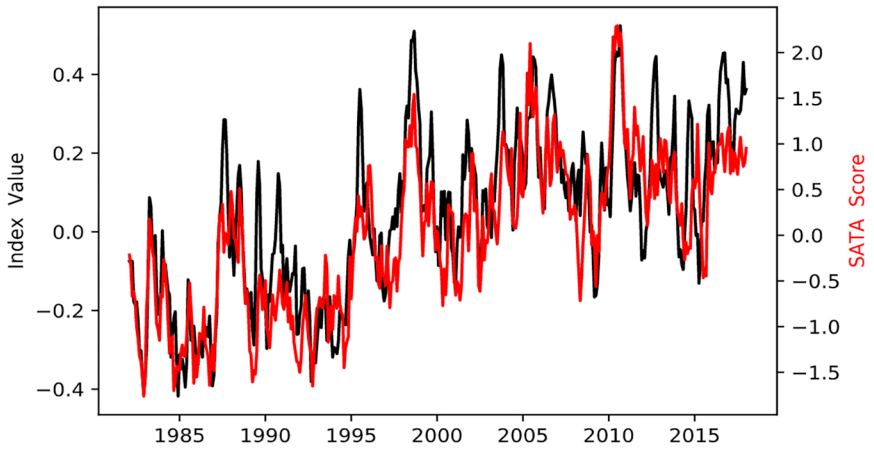

Figure S12. Comparison of the component score for SC2 (red) with the Atlantic Multidecadal Oscillation (black).

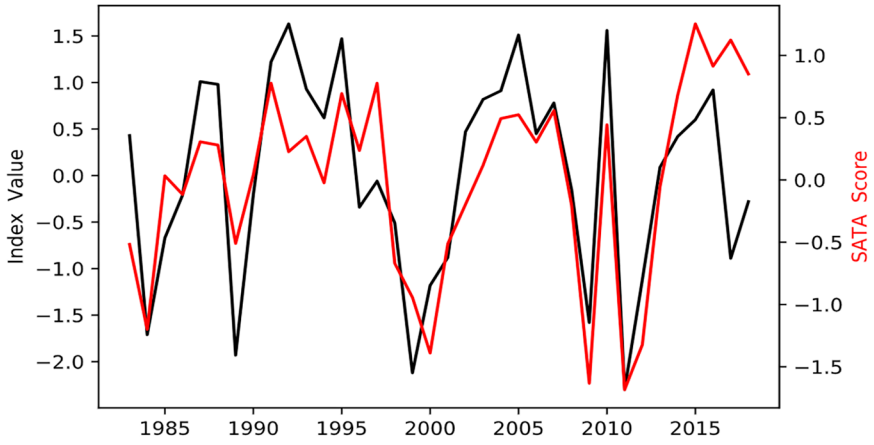

Figure S13. Comparison of the component score for SC3 (red) with the Modoki II Index (black). Note that the Modoki II index is one value per year for the September, October, and November (SON) autumn period. SON averages for SC3 are plotted for comparison.

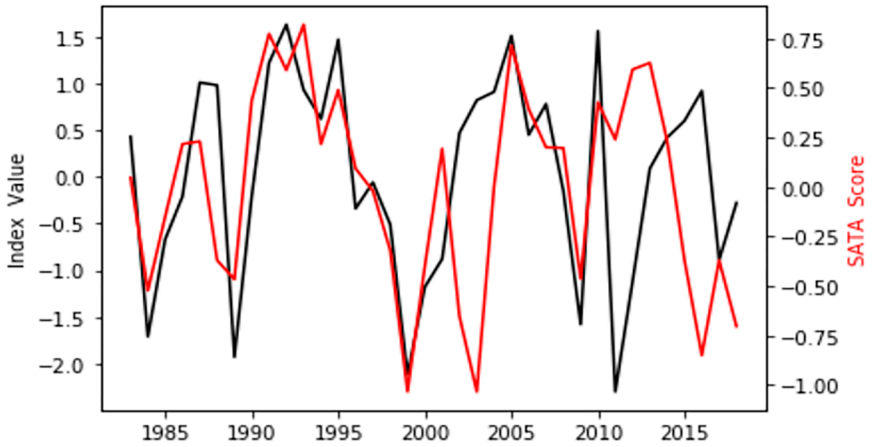

Figure S14. Comparison of the component score for SC4 (red) with the Modoki II Index (black). Note that the Modoki II index is one value per year for the September, October, and November (SON) autumn period. SON averages for SC4 are plotted for comparison.

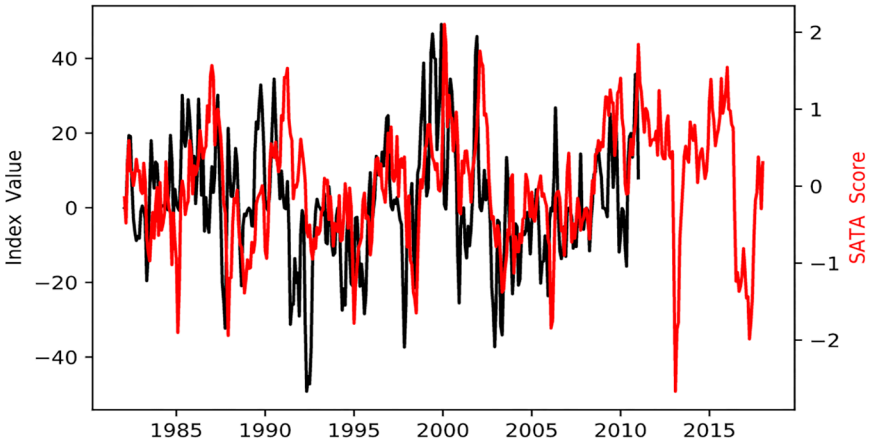

Figure S15. Comparison of the component score for SC5 (red) with the Antarctic Dipole Index (black). Note that the Antarctic Dipole Index only extends from 1982 to 2010.

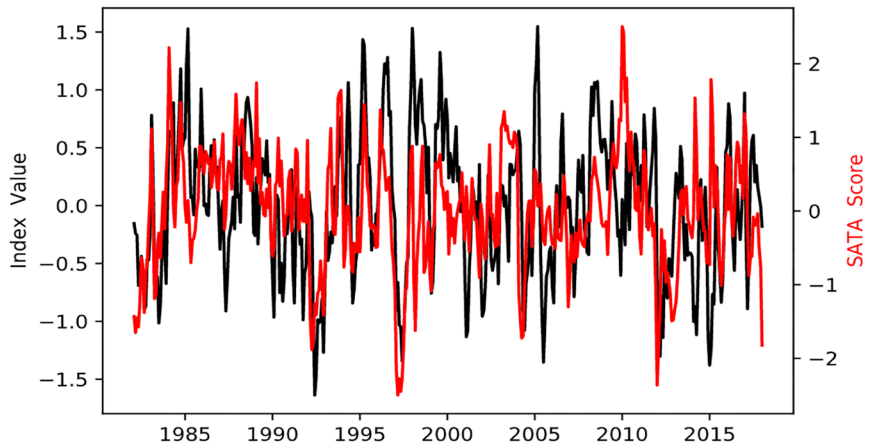

Figure S16. Comparison of the component score for SC6 (red) with the South Atlantic Ocean Dipole (black).

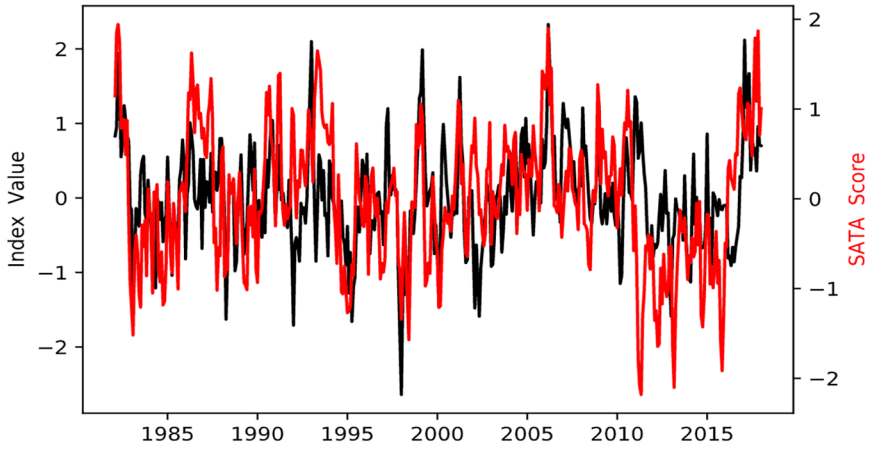

Figure S17. Comparison of the component score for SC7 (red) with the Subtropical Indian Ocean Dipole (black).

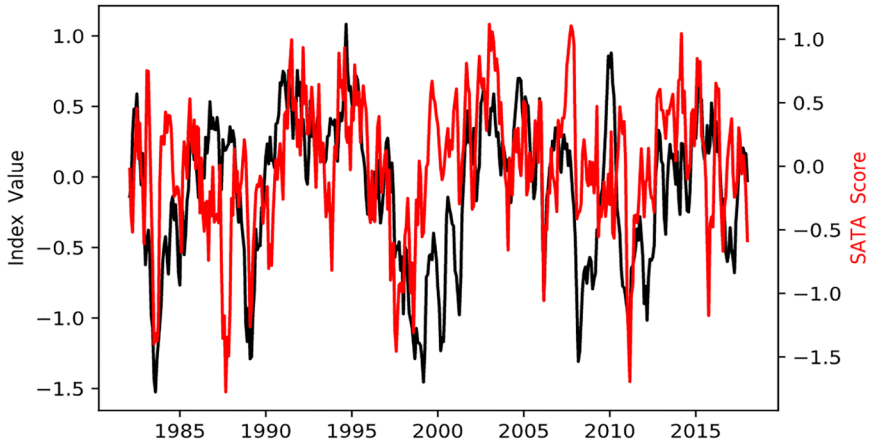

Figure S18. Comparison of the component score for SC8 (red) with the ENSO Modoki Index (black).

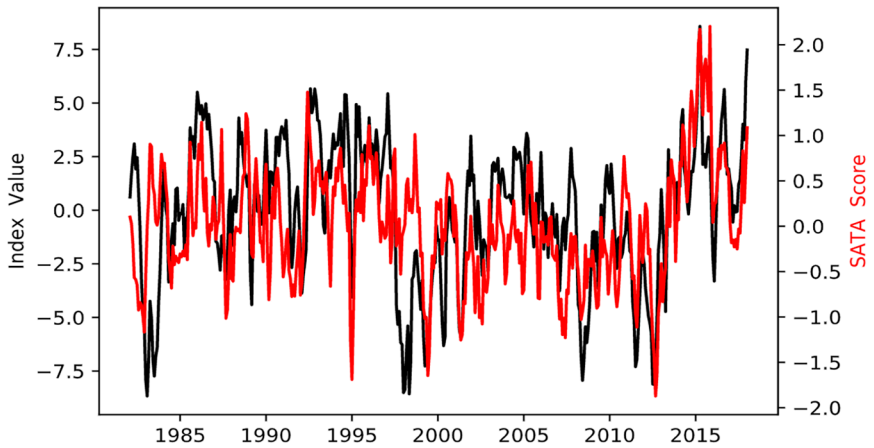

Figure S19. Comparison of the component score for SC9 (red) with the Pacific Meridional Mode (black).

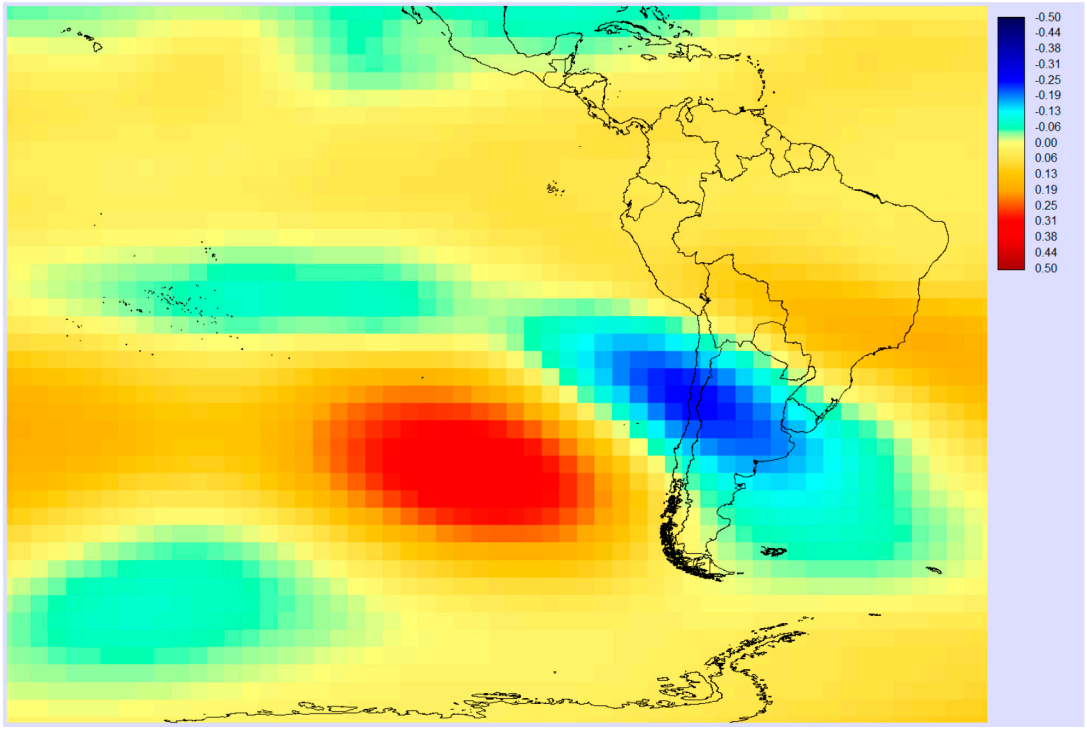

Figure S20. Correlation between SATA Component 10 and monthly anomalies in 500 hPa geopotential heights from 1982 to 2017.